The Trajectory of Sustainable Development

Volume 7, Issue 1, December 2023

Formerly: Journal for Worldwide Holistic Sustainable Development (JWHSD), ISSN2409-9384 (online version) & ISSN 2414-3286 (print version)

Recommended Citation: Aigbokhan, O. J., Adedeji, O. H., Oladoye, A. O., Mshelia, Z. H. (2023). "URBAN LANDSCAPE MORPHOLOGICAL ANALYSIS USING SPATIAL MATRICES. A CASE OF BENIN CITY". The Trajectory of Sustainable Development, 7, 92-115. Available at: https://www.hsdni.org/journal/articles/ .

URBAN LANDSCAPE MORPHOLOGICAL ANALYSIS USING SPATIAL MATRICES. A CASE OF BENIN CITY

Oseyomon John Aigbokhan[1], Oludare Hakeem Adedeji[2], Abiodun Olusegun Oladoye[3] & Zachariah Haruna Mshelia[4]

[1]Department of Environmental Modeling and Biometrics, Forestry Research Institute of Nigeria;

Correspondence email: *oseyomon255@gmail.com*

[2]Department of Environmental Management and Toxicology, College of Environmental Resources Management, Federal University of Agriculture, Abeokuta;

hakeemdare1222@yahoo.com

[3]Department of Forestry and Wildlife Management, College of Environmental Resources Management, Federal University of Agriculture, Abeokuta;

segun11us@yahoo.com

&

[4]Disaster Management Training and Education Centre for Africa, Faculty of Natural and Agricultural Sciences, University of The Free State, Bloemfontein, South Africa;

Mshelia.ZH@ufs.ac.za

Volume 7, Issue 1, December 2023

Formerly: Journal for Worldwide Holistic Sustainable Development (JWHSD), ISSN2409-9384 (online version) & ISSN 2414-3286 (print version)

Abstract

Impervious and building surfaces are currently replacing natural land surfaces and urban vegetation, which has resulted in the creation of various microclimates in both urban and peri-urban locations. This study examines the urban landscape morphological Analysis using spatial matrices, a case of Benin City, deploying geospatial technologies. A classification algorithm called Maximum Likelihood was used on Landsat imagery.Landscape metrics of the study area were calculated using Fragstats 4.2 software. Results of the LULC of 1992 showed that built-up was 19.66%, Bare land 9.25% and area covered by vegetation was 71.08%. In the year 2002, Built-up increased to 23.40%, while bare land and vegetation were 12.43% and 64.16% respectively. In the year 2012 built-up further increased to 44.38%, bare land to 22.20% and vegetation to 33.42%. In 2022 built-up escalated to 61.79%, bare land to 22.29% and vegetation reduced to 15.92%. The overall accuracy of LULC classification for 1992 (95.0%), 2002 (92.2%), 2012 (89.0% and 2022 (89.0%) implied that the algorithm deployed for the classification performed satisfactorily. The number of patches (NumP) of the different LULC types, ranged between 634 and 4697 during the study period, which indicates high landscape fragmentation. For instance, in comparing 2012 to 2022, the number of patches in the bare land class decreased from 3059in the year 2012 to 2937 in the year 2022. The patches within the Built-up land cover also decreased from 1499 to 1210 during the study period.

Keywords: *classification; algorithm; preprocessing; fragmentation*

Volume 7, Issue 1, December 2023
Formerly: Journal for Worldwide Holistic Sustainable Development (JWHSD), ISSN2409-9384 (online version) & ISSN 2414-3286 (print version)

INTRODUCTION

This study discusses the consequences of urbanisation on the land use land cover changes and their attendant fragmentation of the urban landscape (Norton et al., 2015; Bottalico et al., 2016; Pakzad and Osmond, 2016; Aremu et al., 2017). It brings attention to how rapidly urbanisation and population growth have occurred in cities since the Industrial Revolution, altering land use and microclimates. The fact that 70% of the world's population is expected to reside in cities by 2050 was also mentioned (Norton et al., 2015). This will increase urbanisation, landscape fragmentation, biodiversity loss, and climate change vulnerability. Urban landscapes must be thoroughly understood, and geospatial methods must be used, to analyse the spatiotemporal dynamics of urban regions (Wu, 2014). According to the study's findings (Norton et al., 2015), both developed and developing countries are seeing significant urban population growth. This highlights the necessity for sustainable urban development practices.

Understanding changes in land use, natural processes, cultures, and lifestyles can all be better understood by looking at the spatial shapes of an urbanised city. For successful land use planning that makes the most use of available resources, multiple timescales of development pattern analysis can be applied (Olayiwola et al. 2014). As a result, urban studies often focus on the spatial organisation and driving factors behind urban growth and development (Aguilera et al. 2011).In addition, scholars are once again paying attention to how cities are growing into nearby communities (Ferreira et al. 2018; Karg et al. 2019). According to Lawanson et al. (2012) and Adedire (2018), suburban areas serve as a transitional space between urban centres and nearby rural areas. This zone is typically marked by intermittent built-up regions and lower population density in many developing countries.Hence, they are typically referred to as newly urbanised zones (Adedire 2018). Suburban development is brought on by population growth, the suburbanization of the metropolis, a deterioration in the quality of the urban environment, and the ease of obtaining land for construction and commercial use. (Dutta 2012; Appiah et al. 2014). The pull factors in the suburb include improved infrastructure and socio-economic activities and the quest for

Address: 2996 Danforth Avenue, Toronto, Ontario, M4C 1 M7, Canada.

Volume 7, Issue 1, December 2023
Formerly: Journal for Worldwide Holistic Sustainable Development (JWHSD), ISSN2409-9384 (online version) & ISSN 2414-3286 (print version)

affordable housing (Lawanson et al. 2012; Acheampong and Anokye 2013; Appiah et al. 2014). On the whole, there are changes in both the physical processes and human activities in suburban areas (Appiah et al. 2014; Karg et al. 2019).

A platform for examining changes to the landscape through time and place has been made possible by the development of land-change technology, including advancements in GIS and remote sensing (Estoque and Murayama 2015). For instance, the use of spatial metrics to describe the structure of the landscape and the spatiotemporal pattern of landscape modifications is becoming more widely known (Fan and Myint 2014; Estoque and Murayama 2015). According to Shyamantha et al. (2016), spatial metrics are created using fractal geometry and information theory measurements. They stated that to research landscape functions and transformations, one must be able to quantitatively describe the landscape's structure. According to Chen et al. (2016), spatial metrics are a quantitative technique to represent spatial patterns and structures.

Spatial metrics are frequently used in landscape research to find patterns and fragmentation in the landscape (Dezhkam et al. 2017). They are therefore utilised to study the organisation of an area with uniform thematic elements or patches of it (Ferreira et al. 2018). Additionally, the spatial heterogeneity of patches belonging to the same class can be measured using spatial measures (Kumar et al. 2018). Spatial metrics are used in urbanisation studies to evaluate the physical attributes and layout of settlements (Ayila et al. 2014; Wondrade et al. 2014; Rastandeh and Zari 2018). The metrics can be computed as pixel-based indices (such as contagion computed for all pixels in a patch) or as patch-based indices (such as size, shape, edge length, patch density, and fractal dimension) (Singh et al. 2017; Inkoom et al. 2018).

Address: 2996 Danforth Avenue, Toronto, Ontario, M4C 1 M7, Canada.

Volume 7, Issue 1, December 2023
Formerly: Journal for Worldwide Holistic Sustainable Development (JWHSD), ISSN2409-9384 (online version) & ISSN 2414-3286 (print version)

MATERIALS AND METHODS

The Study Area

Benin City, the capital of Nigeria's Edo State, is a pre-colonial city situated between latitudes 6° 23° 55° and 6° 27° N and longitudes 5° 36° 18° and 5° 44° 31° E (Aiyesanmi and Imoisi, 2011). It is divided into three main local government areas, Oredo, Egor, and Ikpoba-Okha, and is thought to cover an area of about 112.552 km2 (Okhakhu, 2010). The geological formation known as the Benin Formation, which dates back to the Miocene and Pleistocene, underlies Benin City. The region is distinguished by a reddish soil surface layer made up of weathered clay and sand particles, and it is encircled by the ancient Benin moats (Odemerho, 1988; Ikhile, 2016). Within the equatorial rainforest zone, the city has a tropical climate with distinct wet and dry seasons. The dry season lasts from December to March, whereas the wet season lasts from mid-April to mid-November. The average annual rainfall in Benin City is from 2000 to 2500 mm, and the average monthly temperature is 28°C (82.40°F). Evergreen rainforests are the dominant vegetation in the region, albeit their extent has decreased due to urbanisation (Ezemonye and Emeribe, 2014).Benin City's geography is low-lying, undulating, and has uneven soils. The western edges gradually slope towards the Ogba Stream, while the eastern portion gently descends towards the Ikpoba River. The soils in the area are made up of a pinkish-yellowish-white layer with various types of sand, gravelly-pebble sands, and clayey soils on top of a lateritic layer of indurated clay and sand that ranges in colour from reddish to reddish-brown.The sedimentary sequences have sporadic clay layers at different depths and are poorly bedded. The Ikpoba and Ovia flood plains also contain alluvium deposits, which are made up of sands, silts, gravels, and organic components (Akujieze, 2004; Eseigbe and Ojeifo, 2012; Ikhine, 2016)

For this study, the US Geological Survey's official website (http://earthexplorer.usgs.gov) provided Landsat satellite imagery from 1992 (TM), 2002 (ETM), 2012 (ETM+), and 2022 (OLI). Except for the thermal IR bands (band 6 for ETM/ETM+ and bands 10 and 11 for OLI sensors), the image pixels were 30 m by 30 m. All

Address: 2996 Danforth Avenue, Toronto, Ontario, M4C 1 M7, Canada.

Volume 7, Issue 1, December 2023
Formerly: Journal for Worldwide Holistic Sustainable Development (JWHSD), ISSN2409-9384 (online version) & ISSN 2414-3286 (print version)

images were taken during the dry season, when satellite views are frequently crisper than during the wet season, to ensure that there were no clouds in the way.The fact that the study's objectives did not place a strong emphasis on seasonality also played a role in the decision to concentrate on the dry season. The Landsat images were collected and georeferenced using the WGS-84 datum, zone 31 North of the Universal Transverse Mercator projection (UTM).Table 1 lists the dates, path/row, and specs for the Landsat TM, ETM+, and OLI images. High-resolution geo-referenced data from Google Earth Imagery (GEI) was also used as a significant information source in addition to Landsat images, particularly in urban areas with complicated land cover patterns. The in-situ data that was used for field validation purposes is shown in Table 1.

The years 1992, 2002, 2012, and 2022 were looked at in this study. ArcGIS 10.4.1, QGIS 3.12, Idrisi Selva 17, Fragstats 4.2.1, and R/RStudio 3.5.2 were among the software utilised. These software systems were chosen because they fit the study's objectives and were relevant to them. ArcGIS 10.4.1 was used to prepare shapefiles and perform vector-related tasks, and QGIS 3.12 was used to preprocess images and assess correctness. Idrisi Selva 17.0 was used for geostatistical analysis, Fragstats 4.2.1 was used to create important landscape measures, and R/RStudio 3.5.2 allowed for extra statistical analysis. With the use of a handheld GPS device, we collected ground control points (GCP).Overall, these tools and techniques made it possible for the study to conduct a complete and trustworthy investigation of UCI and landscape changes.

Image Preprocessing

The pixels in each band of a digital remotely sensed image are found where the rows and columns meet. Equation 1 was used in this investigation to convert the pictures to Top of Atmosphere (TOA) radiance, as explained by Giannini et al. (2015).

$$L\lambda = \left(\frac{\left(L_{MAX}\lambda - L_{MIN}\lambda\right)}{Q_{CAL}\lambda}\right)Q_{CAL} + L_{MIN}\lambda \qquad (1)$$

Where

Address: 2996 Danforth Avenue, Toronto, Ontario, M4C 1 M7, Canada.

Volume 7, Issue 1, December 2023
Formerly: Journal for Worldwide Holistic Sustainable Development (JWHSD), ISSN2409-9384 (online version) & ISSN 2414-3286 (print version)

$L\lambda$ =Spectral radiance at the sensor's aperture [W/(m^2 sr µm)]
Q_{CAL} = Quantized calibrated pixel value [DN]
Q_{CAL}MIN = Minimum quantized calibrated pixel value corresponding to $L_{MIN}\lambda$ [DN]
Q_{CAL}MAX = Maximum quantized calibrated pixel value corresponding to $L_{MAX}\boldsymbol{\lambda}$) [DN]
$L_{MIN}\,\lambda$ = Spectral at-sensor radiance that is scaled to Q_{CAL}MIN [W/(m^2 sr µm)]
LMAX, = Spectral at-sensor radiance that is scaled to Qcalmax [W/ (m 2 sr µm)].

The above expression does not consider the atmospheric effects, therefore there is a need to convert images from radiance to reflectance measures, using equation 2 (Giannini *et al*, 2015).

$$\rho\lambda = \frac{(\pi * TOAr. * d^2)}{E_{SUN}.Cos\theta_{SZ}} \qquad (2)$$

Where;

$\rho\lambda$ = Planetary TOA reflectance (unitless) π= mathematical constant approximately equal to 3.14159 (unitless)
$L\lambda$ = spectral radiance at the sensors aperture [w/(m^2 sr µm)]

d^2 = the earth-Sun distance (Astronomical unit)
E_{SUN} = mean exoatmospheric solar irradiance [w/(m^2 sr µm)]. θ_{SZ}= the solar zenith angle (degree). The sine of the sun's height SE is equal to the cosine of this angle. In other words, SZ = cos (90- SE).

Image Classification

The process of finding and extracting unique classes or themes, such as categories for land use and land cover, from raw digital satellite data received by remote sensing is known as image classification. It is a method for identifying various aspects from a satellite image, such as urban land cover, various types of flora, manmade structures, mineral resources, or changes in any of these qualities (Lillesand et al., 2008).In this work, the supervised classification was applied. For pixel-based supervised classification, the Maximum Likelihood Algorithm was used, and the classification accuracy of the generated images**w**as assessed. A modified version of Mikias et al.'s (2018) classification **scheme (Table 2)** was used to map land use/land cover for the years 1992, 2002, 2012, and 2022 using Landsat data.

Address: 2996 Danforth Avenue, Toronto, Ontario, M4C 1 M7, Canada.

Volume 7, Issue 1, December 2023
Formerly: Journal for Worldwide Holistic Sustainable Development (JWHSD), ISSN2409-9384 (online version) & ISSN 2414-3286 (print version)

The Operation of Maximum Likelihood Classifier

The Maximum Likelihood (ML) approach is a supervised classification method in remote sensing that assumes that all classes have an equal chance of having a pixel in them and that the input bands have a normal distribution. The normal distribution of the data in each band is what is used in machine learning (ML) classification, which might occasionally overclassify signatures with large covariance matrix values.On the other hand, the spectral distance approach establishes the distance between the measurement vector of a candidate pixel and the mean vector of each signature. This method uses the Euclidean distance formula for classification and is computationally effective compared to other supervised approaches. Because it does not account for class variability, it might classify pixels that shouldn't be. The ML technique derives from the Bayes theorem, which creates the posterior distribution P(i|), which denotes the likelihood that a pixel with a feature vector belongs to class i.

$$P(iI\omega) = \frac{P(iI\omega)P(\omega)}{P(\omega)} \quad (3)$$

where

P(ω|i) is the likelihood function,

P(i)is the chance that class i occurs in the study area.It is based on prior information, and

P(ω) is the probability that ω is observed, which can be written as in equation 4.

$$P(\omega) = \sum_{i=1}^{m} P(\omega\ I\ i)\ P(i) \quad (4)$$

where

M is the number of classes.

P(ω) is frequently utilised as a normalisation constant to

Address: 2996 Danforth Avenue, Toronto, Ontario, M4C 1 M7, Canada.

Volume 7, Issue 1, December 2023
Formerly: Journal for Worldwide Holistic Sustainable Development (JWHSD), ISSN2409-9384 (online version) & ISSN 2414-3286 (print version)

$\sum_{i=1}^{m} P(i \mid \omega)$ sums to 1 (Asmala *et al.,* 2012)

Each class in ML classification has an area in multispectral space where its discriminant function is bigger than all other classes. Decision borders split these class regions, and the decision boundary between classes I and j occurs when,

$$g_i(\omega) = g_j(\omega) \quad (5)$$

Accuracy Assessment

Accuracy evaluation, which rates the dependability of image classifications, is crucial for mapping remote sensing data. Errors of omission or commission are typically prevalent in picture classification, resulting in the incorrect classification of specific pixels or groups of pixels. The confusion matrix, sometimes referred to as the error matrix, is often used to demonstrate classification accuracy. The classified map and the reference data are compared at each sample unit; the reference data is represented by columns and the classified map by rows.This matrix illustrates the errors of commission and omission (Pontus, 2013). The Kappa coefficient is widely used to assess the precision of classifications. 400 ground control locations (GCP) are randomly selected each year, and the degree of agreement between the categorised findings and the reference data is evaluated. The error matrix and Kappa coefficient are popular methods for evaluating the accuracy of thematic maps produced during the classification process (equation 6).

$$K_{APPA} = \frac{N\Sigma^{k} X_{ii} \Sigma^{k}\left(X_{i+} \times X_{+i}\right)}{N^{2} - \Sigma^{k}\left(X_{i+} \times X_{+i}\right)} \quad (6)$$

where:

KAPPA = Kappa index,
k = number of matrix files,

Address: 2996 Danforth Avenue, Toronto, Ontario, M4C 1 M7, Canada.

Volume 7, Issue 1, December 2023
Formerly: Journal for Worldwide Holistic Sustainable Development (JWHSD), ISSN2409-9384 (online version) & ISSN 2414-3286 (print version)

Xii = observation number on row i and column I (along the diagonal),
(X_{i+} and X_{+i}) = total marginal for row i and column i, respectively,
N = total number of observations.

Spatial Metrics Analysis

This study employed spatial metrics, such as Number of Patches (NumP), Edge Density (ED), Mean Nearest Neighbour Index (MNN), Fractal Dimension (FDim), Mean Patch Index (MPI), and Mean Patch Size (MPI), to investigate the spatial heterogeneity of classes and examine changes in urban growth patterns. Urban fragmentation was measured and analysed using the FRAGSTATS programme, and themed maps that depict spatial patches were produced. When choosing the best spatial metrics, the study took into account both the temporal scale and the harmonic oscillation behaviour of the measures (Ekwe, 2018).Not all spatial measures assess the same characteristics of spatial patterns, and some of them may even exhibit substantial correlation and redundancy (McGarigal and Marks, 1995). Previous studies have demonstrated how to use specific metrics to evaluate urban growth patterns, and the findings indicate that while some metrics exhibit harmonic oscillation across the research period, others do not (Dietzel et al., 2005).

Number of Patches (NP):When the landscape only contains one patch of the matching patch type, or when the class only consists of one patch, NP is equal to 1. The number of patches of the respective patch type is represented by NP (McGarigal et al, 1995).

$$NP = n_i \quad (8)$$

Mean Patch Index (MPI):MPS equals the sum of the areas (m^2) of all patches of the corresponding patch type, divided by the number of patches of the same type, divided by 10,000 (to convert to hectares). The minimum patch size, image extent, and grain in MPS all limit the range in a similar way to how patch area does (AREA). MPI units in hectares (McGarigal *et al*, 1995).

Address: 2996 Danforth Avenue, Toronto, Ontario, M4C 1 M7, Canada.

Volume 7, Issue 1, December 2023

Formerly: Journal for Worldwide Holistic Sustainable Development (JWHSD), ISSN2409-9384 (online version) & ISSN 2414-3286 (print version)

$$MPS = \frac{\sum_{k=i}^{m} A_k}{m} \quad (9)$$

Mean Nearest-Neighbour Distance:MNN equals the sum of the distance (m) to the nearest neighbouring patch of the same type, based on the nearest edge-to-edge distance, for each patch of the corresponding patch type, divided by the quantity of identical-type patches. MNN unit is in meters (McGarigal *et al*, 1995).

$$MNN = \frac{\sum_{j=1}^{n} h_{ij}}{n_i} \quad (10)$$

***Mean Proximity Index (MPI)*:** If there are no neighbours of the same type in the specified search radius for any patches of the corresponding patch type, MPI is equal to 0. When the linked patch type's distribution is less fragmented and the relevant patches are less isolated, MPI increases. The search radius and the smallest separation between patches were used to estimate the upper limit of MPI. MPI is the same as the class's mean proximity index for patches. When the search buffer crosses the landscape boundary for focal patches close to the boundary, it should be noted that only patches within the landscape are considered in the computations. There is one fewer unit (McGarigal et al., 2012).

$$the\ MPI = \frac{\sum_{j=is=i}^{n}\sum^{n} \frac{a_{ijs}}{h_{ijs}^2}}{n_i} \quad (11)$$

Fractal Dimension (FDim): By multiplying the logarithm of patch area (m2) by the logarithm of patch perimeter (m), the FDim metric is calculated. This is carried out for each patch of the relevant patch type, and the total number of patches of that type is then divided. The bias in the perimeter is then addressed by altering the raster calculation.

$$FDim = \frac{\sum_{J=1}^{N}\left(\frac{2\,In(025P_y}{ina_y}\right)}{n_1} \quad (12)$$

Address: 2996 Danforth Avenue, Toronto, Ontario, M4C 1 M7, Canada.

Volume 7, Issue 1, December 2023

Formerly: Journal for Worldwide Holistic Sustainable Development (JWHSD), ISSN2409-9384 (online version) & ISSN 2414-3286 (print version)

For a 2-dimensional landscape mosaic, a fractal dimension larger than 1 denotes a departure from Euclidean geometry (i.e., a rise in patch shape complexity). This comes close to 1 for shapes with extremely straightforward perimeters, such as squares or circles, and comes close to 2 for shapes with complicated, plane-filling perimeters.

Edge Density (ED): The lengths of all edge segments connected to a specific patch type are added up to create the ED metric, which is expressed in metres. To translate this figure to hectares, divide it by the total area of the landscape (calculated in square metres), and then multiply the result by 10,000. If a border is present in the landscape, only those boundary segments that are true edges and are connected to the relevant patch type are included in the ED calculation.

$$ED = \frac{\sum_{K=1}^{N} e_{ik}}{A}(10,000) \quad (13)$$

ED $\geq$ 0, without limit
ED = 0 when there is no class edge in the landscape

RESULTS AND DISCUSSION

Land use Land cover Distribution

Address: 2996 Danforth Avenue, Toronto, Ontario, M4C 1 M7, Canada.

Volume 7, Issue 1, December 2023
Formerly: Journal for Worldwide Holistic Sustainable Development (JWHSD), ISSN2409-9384 (online version) & ISSN 2414-3286 (print version)

The land use and land cover (LULC) analysis for the study area between 1992 and 2022 revealed significant changes (Figure 2). From 19.66% in 1992 to 61.79% in 2022, the built-up area increased steadily, illustrating urban renewal and growth. Conversely, vegetation cover decreased from 71.08% in 1990 to 15.92% in 2022, while bare land increased from 9.25% to 22.29% within the same period. Between 1992 and 2002, the built-up land cover changed by 3.74%; by 2022, it will have increased by 17.41%. Vegetation changed by 6.92% between 1992 and 2002, then by 30.74% between 2002 and 2012, before decreasing to 17.5% in 2022. The spatial distribution of LULC classes supported the statistics shown in Tables 3 and 4.

Accuracy Assessment of the Classified Images

The degree of accuracy of the categorised imageswas evaluated using the accuracy assessment method from Erdas Imagine 2014. For the accuracy evaluation, 400 sample points were used for the analysis. The technique compares only reference pixels with well-known class names to the pixels in the thematic data layer. Table 5 displays the report summary following the application of the method. For the 1992 LULC, the built-up area accuracy (Pa) and user accuracy (Ua) are 93.8%, 92.9%, 91.3%, and 76.3% for bare land and 96.0%, 98.8% for vegetation, respectively. In 2022, the Pa and Ua will be built-up (87.7%, 97.8%), bare land (96.3%, 78.1%), and vegetation (83.7%, 77.9%), respectively. These levels of precision are acceptable and sufficient. According to the "overall accuracy" of the LULC classification for 1992 (95.0%), 2002 (92.2%), 2012 (89.0%), and 2022 (89.0%), the LULC classification employed in this study is satisfactory.

Changes in landscape patterns

The alteration of the landscape in Benin City between 1992 and 2022 was investigated using land use classes and geographical indicators (Table 6). There was significant fragmentation, particularly in the category of barren land. Over time, there were fewer areas of developed areas and more bare ground. The edge density and patch count showed a strong association. The mean patch size in 1992 revealed higher vegetation cover

Address: 2996 Danforth Avenue, Toronto, Ontario, M4C 1 M7, Canada.

Volume 7, Issue 1, December 2023
Formerly: Journal for Worldwide Holistic Sustainable Development (JWHSD), ISSN2409-9384 (online version) & ISSN 2414-3286 (print version)

fragmentation. In 2022, this pattern started to change. The fractal dimension remained mostly consistent throughout the investigation. The mean patch index was higher in built-up regions in 2022. Greater class patch dispersion was shown to exist based on the average distance to the closest neighbour. This shows that the conversion of other land use classes throughout the period from 1992 to 2022 resulted in a remarkable expansion rate. These landscape indicators reveal urban expansion and fragmentation.

Results of similar studies revealed that the development pattern was not uniform in all directions and varied with the availability of space for expansion (Toyobo et al. 2011; Agbor et al. 2012; Adegboyega and Aguda 2016).

CONCLUSION AND RECOMMENDATIONS

This study uses remote sensing and GIS to evaluate the land use and land cover of Benin City. Anthropogenic activities were identified to be the primary driving elements behind LULC dynamics. The proportion of built-up areas climbed from 23.40% to 44.38% between 2002 and 2012, and then increased once more to 61.79% in 2023. Urbanisation reduced the vegetation cover to 17.5% by 2023. The Markov Chains method was used to predict the LULC for 2032, and the results showed a net shift of 9942 ha from bare land and vegetation to built-up areas. The accuracy evaluation showed that the classification had acceptable levels of accuracy.

The prevalence of patches in both populated and bare areas implied fragmentation since bare land is in transition. Less barren land patches existed between 1992 and 2023. Therefore, it is advised that governments (local and state) pay greater attention to the causes of urban fragmentation to control further fragmentation of the cityscape in light of the study's findings. Second, governments, non-governmental organisations, and community-based advocacy groups must start planting trees in open places around the city because the LULC projection for the year 2032 revealed that a large amount of the city's green spaces will be turned into impermeable spaces.

REFERENCES

Acheampong, RA, & Anokye, PA, (2013). Understanding households'

Volume 7, Issue 1, December 2023

Formerly: Journal for Worldwide Holistic Sustainable Development (JWHSD), ISSN2409-9384 (online version) & ISSN 2414-3286 (print version)

residential location choice in Kumasi's peri-urban settlements and the implications for sustainable urban growth Research. *Humanities and Social Sciences,* 3(9), 60–70.

Adedire, FM, (2018). Peri-urban Expansion in Ikorodu, Lagos: Extent, Causes, Effects, and Policy Response.*Urban Forum*, 29(3), 259-275.

Adegboyega, SA and Aguda, AS, (2016). Spatio-temporal analysis of urban sprawl in a fringe area around Ibadan, Southwestern Nigeria'.*Ife Research Publications in Geography*, 9(1), 132-154.

Agbor, CF, Aigbokhan, OJ, Osudiala, CS & Malizu, L, (2012). Land use land cover change prediction of Ibadan metropolis'.*Journal of Forestry and Environment,* 9, 1-13

Aiyesanmi, A. F. and Imoisi, O. B. (2011). Understanding Leaching Behaviour of Landfill Leachate in Benin City, Edo State, Nigeria through Dumpsite Monitoring. *British Journal of Environment & Climate Change,* 1(4), 190-200.

Akujieze, C. N. (2004). Effects of Anthropogenic Activities (Sand Quarrying and Waste Disposal) on Urban Groundwater System and Aquifer Vulnerability Assessment in Benin City, Edo State, Nigeria. PhD Thesis, University of Benin, Benin City, Nigeria.

Appiah, D. O., Bugri, J. T., Forkuo, E. K., Boateng, P. K. (2014). Determinants of peri-urbanization and land use change patterns in peri-urban Ghana. *Journal of Sustainable Development*, 7(6), 96–106.

Asmala, A. and Shaun, Q. (2012). Analysis of Maximum Likelihood Classification on Multispectral Data. *Applied Mathematical Sciences,* 6(129), 6425 – 6436.

Ayila, AE, Oluseyi, FO, & Anas, BY, 2014, 'Statistical Analysis of Urban Growth in Kano Metropolis, Nigeria'.*International Journal of Environmental Monitoring and Analysis,* 2(1), 50-56.

Bottalico, F., Chirici, G., Giannetti, F., DeMarco, A., Nocentini, S., Paoletti, E., Salbitano, F., Sanesi, G., Serenelli, C. and Travaglini, D. (2016). Air Pollution Removal by Green Infrastructures and Urban Foresta in the City of Florence. *Agriculture and Agricultural Science Procedia*. 8, 243-251.

Chen, A, Zhao, X, Yao, L & Chen, L, (2016). Application of a new integrated landscape index to predict potential urban heat islands'.*Ecological Indicators*, 69, 828-835.

Dezhkam, S, Jabbarian Amiri, B, Darvishsefat, AA and Sakieh, Y, (2017). Performance evaluation of land change simulation models using landscape metrics'.*Geocarto international,* 32(6), 655-677.

Dietzel, C., Oguz, H., Hemphill, J. J., Clarke, K. C. and Gazulis, N. (2005). Diffusion and Coalescence of the Houston metropolitan area: Evidence supporting a new urban theory. *Environmental. Planning* B, 32, 231–246.

Volume 7, Issue 1, December 2023

Formerly: Journal for Worldwide Holistic Sustainable Development (JWHSD), ISSN2409-9384 (online version) & ISSN 2414-3286 (print version)

Dutta, V, (2012) Land use dynamics and peri-urban growth characteristics: reflections on master plan and urban suitability from a sprawling north Indian city'.*Environment and Urbanization ASIA*, 3(2),277–301.

Ekwe, M. C., Adedeji, O. I., Ahmad, A. and Joshua, J. K. (2018). Assessment of green parks cooling effect on Abuja urban microclimate using geospatial techniques. *Remote Sensing Applications*: *Society and Environment* 11, 11-21.

Eseigbe, J. O. and Ojeifo, M. O. (2012). Aspects of Gully Erosion in Benin City, Edo State, Nigeria. *Research on Humanities and Social Sciences* 2(7),45- 66

Estoque, RC & Murayama, Y, 2015, 'Intensity and spatial pattern of urban land changes in the megacities of Southeast Asia'.*Land Use Policy*, 48, 213–222.

Ezemonye, M. N. and Emeribe, C. N. (2014). Flooding and Household Preparedness in Benin City, Nigeria. *Mediterranean Journal of Social Sciences,* 5(1), 547.

Fan, C & Myint, SA, 2014, 'Comparison of spatial autocorrelation indices and landscape metrics in measuring urban landscape fragmentation'.*Lands. Urban Plan.*, 121, 117–128.

Ferreira, IJM, Ferreira, JHD, Bueno, PAA, Vieira, LM, de Oliveira Bueno, R and do Couto, EV, (2018). Spatial dimension landscape metrics of Atlantic Forest remnants in Paraná State, Brazil', *Acta Scientiarum. Technology*. 40(1),1-8.

Giannini, M. B., Belfiore, O. R., Parente, C. and Santamaria, R.(2015). Land Surface Temperature from Landsat 5 TM images: comparison of different methods using airborne thermal data measurements and comparison with MODIS remote sensing estimates." *Agricultural and Forest Meteorology*. 129, 151- 173.

Ikhile, C. I. (2016). Geomorphology and Hydrology of the Benin Region, Edo State, Nigeria. *International Journal of Geosciences*, 7, 144-157

Inkoom, JN, Frank, S, Greve, K, Walz, U & Furst, C, (2018). Suitability of different landscape metrics for the assessments of patchy landscapes in West Africa'.*Ecological Indicators*, 85,117-127.

Karg, H, Hologa, R, Schlesinger, J, Drescher, A, Kranjac-Berisavljevic, G, Glaser, R, (2019). 'Classifying and Mapping Periurban Areas of Rapidly Growing Medium-Sized Sub-Saharan African Cities: A Multi-Method Approach Applied to Tamale, Ghana', Land, 8(3), 40.

Kumar, M, Denis, DM, Singh, SK, Szabo, S and Suryavanshi, S, (2018). 'Landscape metrics for assessment of land cover change and fragmentation of a heterogeneous watershed'.*Remote Sensing Applications: Society and Environment,* 10, 224-233.

Lawanson, T, Yadua, O, Salako, I, (2012). 'An investigation of rural-urban

Volume 7, Issue 1, December 2023

Formerly: Journal for Worldwide Holistic Sustainable Development (JWHSD), ISSN2409-9384 (online version) & ISSN 2414-3286 (print version)

linkages of the Lagos megacity, Nigeria'.*Journal of Construction Project Management and Innovation,* 2(2), 464–581.

Lillesand, T. M. and Kiefer, R. Remote Sensing Image Interpretation. John Wiley, New York. 2008.

McGarigal, K, Cushman, SA, Neel, MC, Ene, E, 2002, FRAGSTATS: spatial pattern analysis program for categorical maps, Computer Software Program, University of Massachusetts, Amherst, viewed 29 April 2019. http://www.umass.edu/landeco/research/fragstats/fragstats.html

McGarigal, K. and Marks, B. J. (1995). FRAGSTATS: Spatial pattern analysis program for quantifying landscape structure. Gen. Tech. Rep. PNW-GTR-351. U.S. Department of Agriculture, Forest Service, Pacific Northwest Research Station. Portland OR. 122.

Mikias, B., Molla, I. C. O. and Olatubara (2018). The Spatio-Temporal Pattern of Urban Green Spaces in Southern Ethiopia. *American Journal of Geographic Information System.* 7(1): 1-14.

Norton, T. A., Hannes, Z., Stacey, L. P. and Neal, M. P.(2015). Bridging the Gap between Green Behavioural Intensions and Employee Green Behaviour: The Role of Green Psychological Climate. *Journal of OrganizationalBehaviour* 38(7).

Odemerho, F. O. Benin City: A Case Study of Urban Flood Problems. In Sada, P.O. and Odemerho, F. O. (Eds). (1988). Environmental Issues and management in Nigerian Development, Evans Brothers, Ibadan.

Okhakhu, P. A. The Significance of Climatic Elements in Planning the Urban Environment of Benin City, Nigeria. Unpublished PhD Thesis. Ekpoma-Nigeria: Department of Geography and Regional Planning, Ambrose Alli University. 2010.

Olayiwola, AM, Ajala, OA & Sangodipe, JA, (2014). 'Physical Growth Pattern of Settlements in a Traditional Region, Southwest Nigeria'.*International Journal of Geosciences,* 5, 1345-1360.

Pakzad, P. and Osmond, P. Corrigendum for developing a sustainability indicator sets for measuring green infrastructure performance. *Procedia – Social and Behavioural sciences* 2, 16. 2016.

Rastandeh, A & Zari, MP, (2018). A spatial analysis of land cover patterns and its implications for urban avifauna persistence under climate change'.*Landscape Ecology,* 33(3),455-474.

Shyamantha, S, Ronald, CE & Yuji, M, 2016, 'Spatiotemporal Analysis of Urban Growth Using GIS and Remote Sensing: A Case Study of the Colombo Metropolitan Area, Sri Lanka.*International Journal of Geo-Information* 5, (11), 1-19.

Singh, SK, Srivastava, PK, Szabo, S, Petropoulos, GP, Gupta, M & Islam, T, (2017). Landscape transform and spatial metrics for mapping spatiotemporal land cover dynamics using Earth Observation data-sets.*Geocarto international*, 32 (2), 113-127.

Volume 7, Issue 1, December 2023

Formerly: Journal for Worldwide Holistic Sustainable Development (JWHSD), ISSN2409-9384 (online version) & ISSN 2414-3286 (print version)

Toyobo, AE, Muili, AB & Adetunji, MA, (2011). The Relevance of Infrastructural Facilities to Rural Housing Development in Lagelu Local Government, Oyo State, Nigeria'. *International NGO Journal,* 9(3), 29-34.

Wondrade, N, Dick, OB, & Tveite, H, (2014) Landscape mapping to quantify degree-of-freedom, degree-of-sprawl, and degree-of-goodness of urban growth in Hawassa, Ethiopia'.*Environment and Natural Resources Research*, 4 (4),223-237.

Wu, J. (2014).Urban ecology and Sustainability: The State of the science and future directions. *Landscape and Urban Planning*, 125, 209-221.

Volume 7, Issue 1, December 2023
Formerly: Journal for Worldwide Holistic Sustainable Development (JWHSD), ISSN2409-9384 (online version) & ISSN 2414-3286 (print version)

Appendix

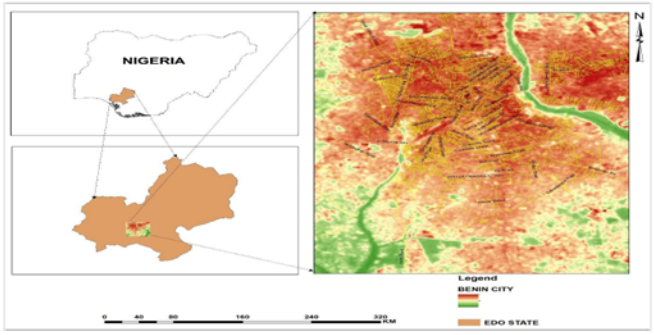

Figure 1: Map of the study area in Edo state, Nigeria.

Table 1: Satellite Images and their acquisition date.

Satellite Sensor	**Spatial resolution**	**Acquisition years**	**Path**	**Row**	**Source**
Landsat TM, ETM, ETM+ and OLI	30m x 30m	January 4th,1992, February 7th,2002, February 3rd, 2012 March 7th, 2022	189	56	https: earthexplorer.usgs.gov
Google Earth Imagery	2.5m x 2.5m	1992, 2002, 2012 and 2022	-	-	Google Earth Pro
SRTM image	30m x 30m				https: earthexplorer.usgs.gov

Address: 2996 Danforth Avenue, Toronto, Ontario, M4C 1 M7, Canada.

Volume 7, Issue 1, December 2023
Formerly: Journal for Worldwide Holistic Sustainable Development (JWHSD), ISSN2409-9384 (online version) & ISSN 2414-3286 (print version)

Table 2: A land use land cover classification scheme

Built-up area	The urban area according to studies is made up of impervious pavement, such as roads, concrete, and walkways, as well as structures seen in the urban setting. The region also has green spaces, which are areas of land that are partially or entirely covered in vegetation like grass, trees, shrubs, or other kinds of plants.
Vegetated area	Green space consists of public parks, neighbourhood gardens, plantation and natural forests, greenways, green areas, institutional grounds, cemeteries, and religious grounds.
Bare land	Remnant parcels, which are often small in size, frequently spherical, and have not been developed in the past; parcels with physical restrictions, such as a high slope or a flood hazard, and which are therefore inevitable; or reserve parcels maintained for future relocation and enlargement.

Source: Mikias *et al.* (2018)

Address: 2996 Danforth Avenue, Toronto, Ontario, M4C 1 M7, Canada.

Volume 7, Issue 1, December 2023

Formerly: Journal for Worldwide Holistic Sustainable Development (JWHSD), ISSN2409-9384 (online version) & ISSN 2414-3286 (print version)

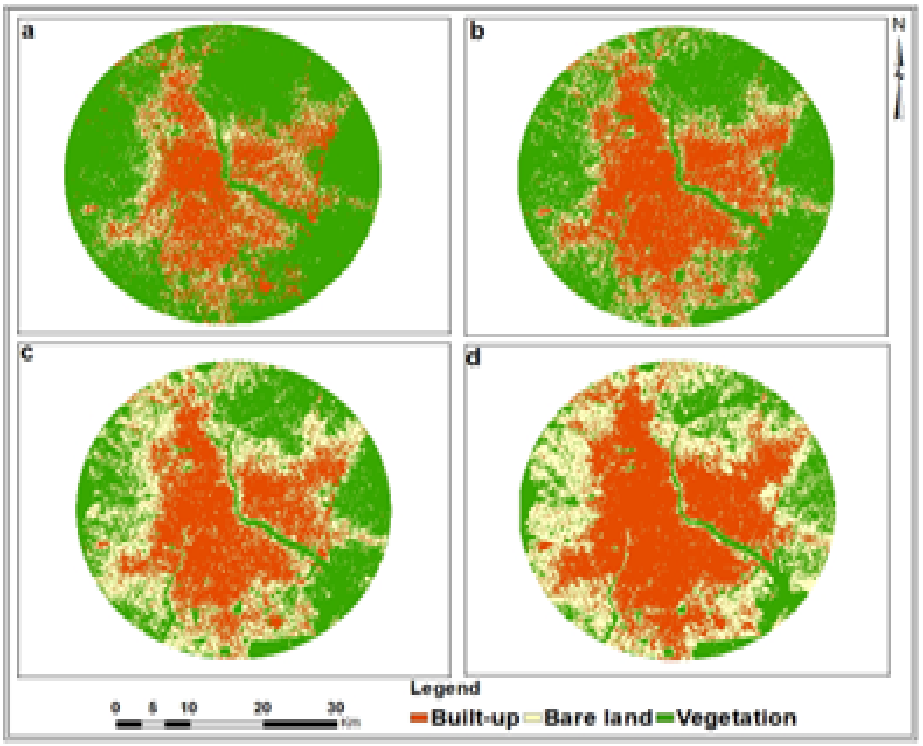

Figure 2: Land Use Land Cover Map of Benin City in (a)1992, (b) 2002, (c) 2012) and (d)2022

Table 3: LULC statistics for the study area.

	1992		2002		2012		2023	
LULC	Area(ha)	%	Area(ha)	%	Area(ha)	%	Area(ha)	%
BU	14798.97	19.66	17615.70	23.40	33399.27	44.38	46504.08	61.79
BL	6964.38	9.25	9358.29	12.43	16710.21	22.20	16778.16	22.29
VEG	53502.48	71.08	48291.84	64.16	25156.35	33.42	11983.59	15.92

BU = Built-up, *BL = Bare land, *VEG = Vegetation

Address: 2996 Danforth Avenue, Toronto, Ontario, M4C 1 M7, Canada.

Volume 7, Issue 1, December 2023
Formerly: Journal for Worldwide Holistic Sustainable Development (JWHSD), ISSN2409-9384 (online version) & ISSN 2414-3286 (print version)

Table 4: LULC change of Benin City and its environs

LULC	1992-2)02		2002-2 012		2012- 2022	
	Area (Δ *ha*)	(Δ%)	Area (Δ *ha*)	(Δ%)	Area (Δ *ha*)	(Δ%)
Built Up	2816.73	3.74	15783.57	20.98	13104.81	17.41
Bare Land	2393.91	3.18	7351.92	9.77	67.95	0.09
Vegetation	-5210.64	-6.92	-23135.49	-30.74	-13172.76	-17.5

Table 5: Summarized statistics of accuracy assessment

Class Name	**1992** [illegible]	**2002** [illegible]	**2012** [illegible]	**2022** [illegible]
Built Up	93.8, 92.9	86.3, 90.9	87.3, 94.1	87.7, 97.8
Bare land	91.3, 76.3	95.1, 72.8	97.2, 78.8	96.3, 78.1
Vegetation	96.0, 98.8	93.7, 97.7	85.6, 91.0	83.7, 77.9
Overall accuracy	**95.0**	**92.2**	**89.0**	**89.0**
Kappa Statistics	**89.5**	**85.3**	**83.1**	**80.6**

Pa = Producer accuracy *Ua = User accuracy

Table 6: Metrics Values for each Landscape type between 1992 and 2022

Address: 2996 Danforth Avenue, Toronto, Ontario, M4C 1 M7, Canada.

Volume 7, Issue 1, December 2023

Formerly: Journal for Worldwide Holistic Sustainable Development (JWHSD), ISSN2409-9384 (online version) & ISSN 2414-3286 (print version)

Date	LULC class			METRICS			
1992	LULC	NumP	ED	MPS	FDim	MPI	MNN
	Built-Up	1022	11.47	14.48	1.03	9533.36	140.84
	Bare Land	3006	31.71	2.32	1.04	553.91	99.33
	Vegetation	456	23.42	117.33	1.03	137347.3	82.57
2002	LULC	NumP	ED	MPS	FDim	MPI	MNN
	Built-Up	920	19.39	19.15	1.04	18542.57	141.64
	Bare Land	4687	41.16	2.0	1.04	133.11	85.21
	Vegetation	774	31.53	62.39	1.03	43681.33	92.21
2012	LULC	NumP	ED	MPS	FDim	MPI	MNN
	Built-Up	1499	28.86	22.28	1.03	44606.56	99.41
	Bare Land	3059	53.53	5.46	1.04	2120.8	86.88
	Vegetation	960	26.45	26.2	1.04	9671.45	80.15
2022	LULC	NumP	ED	MPS	FDim	MPI	MNN
	Built-Up	1210	34.47	38.43	1.03	66851.97	81.56
	Bare Land	2937	48.04	5.71	1.04	2057.83	87.69
	Vegetation	634	14.3	18.9	1.04	3463.27	125.27

Address: 2996 Danforth Avenue, Toronto, Ontario, M4C 1 M7, Canada.